Keto-enol tautomerization drives the self-assembly of Leucoquinizarin on Au(111).

Roberto Costantini, Luciano Colazzo, Laura Batini, Matus Stredansky, Mohammed S. G. Mohammed, Simona Achilli, Luca Floreano, Guido Fratesi, Dimas G. de Oteyza and Albano Cossaro

Supporting Information

1. Materials and methods

Experimental.

The LQZ powder was purchased from TCI (purity >98%) and sublimated from a Knudsen cell at 370K. Deposition was performed at room temperature. The Au(111) sample was cleaned by cycles of Ar+ sputtering and annealing at 800 K.

O1s and C1s XPS were measured at 650 eV and 515 eV with overall resolution of 0.25 eV and 0.2 eV respectively. Binding energy calibration was done by measuring the $Au4f_{7/2}$ peak and by aligning its bulk component to 84.0 eV[1]. NEXAFS spectra were acquired in Auger yield measuring the Auger signal at 252 eV and 507 eV respectively.

STM measurements have been performed at the *Donostia* International Physics Center on a commercial Scienta-Omicron LT-SPM system at 4.3 K. A mechanically clipped PtIr wire was used as tip, sharpened by voltage pulses and indentation into clean Au(111) patches. The images were analysed with the WSxM software.[2]

Calculations.
We performed the theoretical analysis based on density functional theory (DFT) simulations within the Perdew-Burke-Ernzerhof (PBE) approximation to the exchange-correlation functional[3], using the Quantum-ESPRESSO simulation package[4] and the same norm-conserving pseudopotentials and numerical setup as in our previous studies[5]. Free molecules have been optimized in periodically repeated orthorhombic cells with a vacuum separation between replicas of 11 Å. We evaluate core-level spectra as described elsewhere.[6] Self-consistent calculations with a C pseudopotential generated with a 1s full core hole (FCH)[7] at a given atom site provide the XPS core level shifts between inequivalent carbon (oxygen) atoms: those range from C01 to C07 (O01 to O02) for tautomers T0, T1, and T2, and up to C14 (O04) for T3. Next, we evaluate NEXAFS within the half-core-hole approach (HCH) [8,9] by using the xspectra code[10]. Within a pseudopotential approach, the XPS and NEXAFS spectra of the molecule are both defined up to an energy constant, which is adjusted to match the experimental features.

2. STM imaging

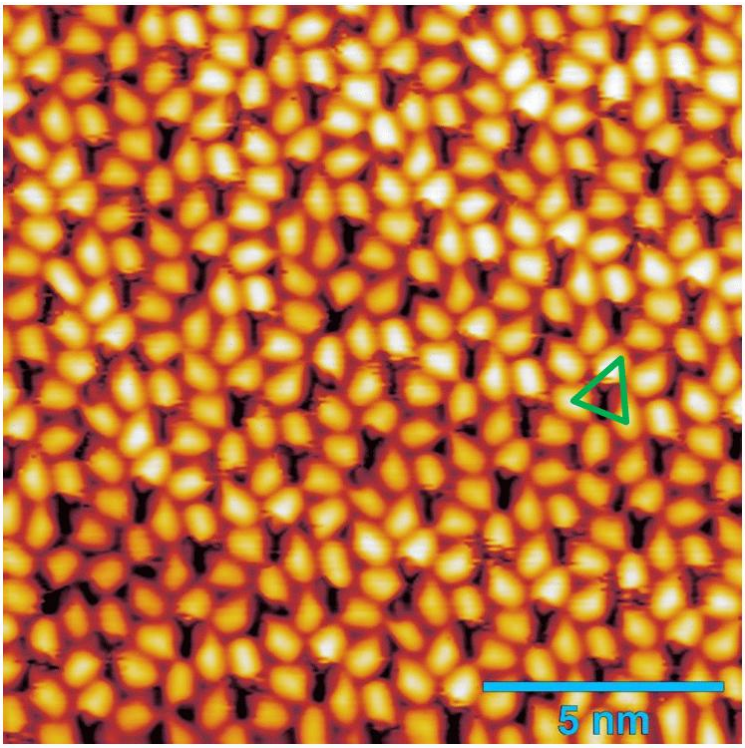

Figure S1 The RT growth of the monolayer of LQZ leads to less ordered phases with respect to the honeycomb structure presented in the manuscript. As shown in the image, a quite compact assembly of molecules is formed, where molecular trimers similar to the ones discussed in the manuscript, exhibiting a more distorted geometry, can be identified (green triangle). STM parameters: 0.03 V, 200 pA.

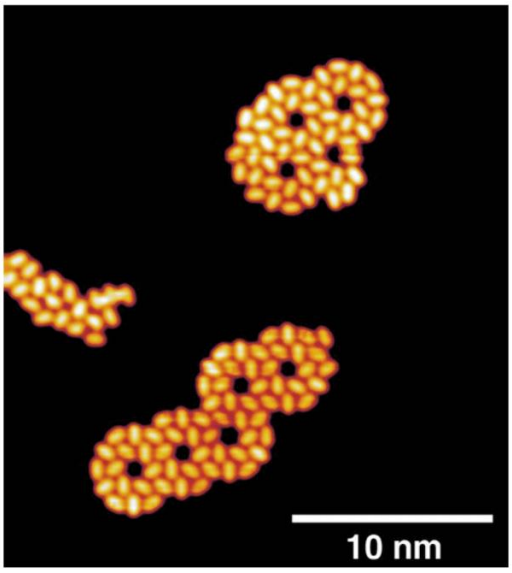

Figure S2. Thermal treatment of the LQZ films reveald that the desorption of the molecules is obtained at sample temperature Ts~500K. Image shows a very low coverage film, obtained upon annealing of a submonolayer at 420K, where both chiralities of the pores are present.(0.05 V, 100 pA).

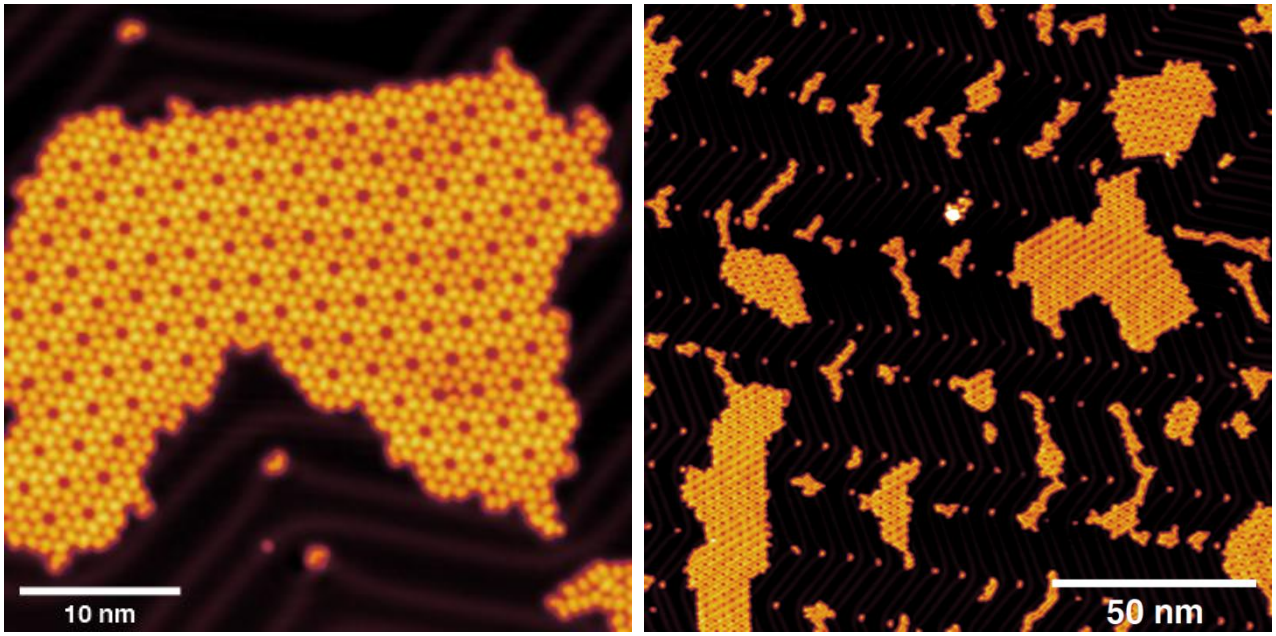

Fig S3 Two large scale images of the porous phase presented in the manuscript (0.4V, 20pA).

3. Telegraph noise

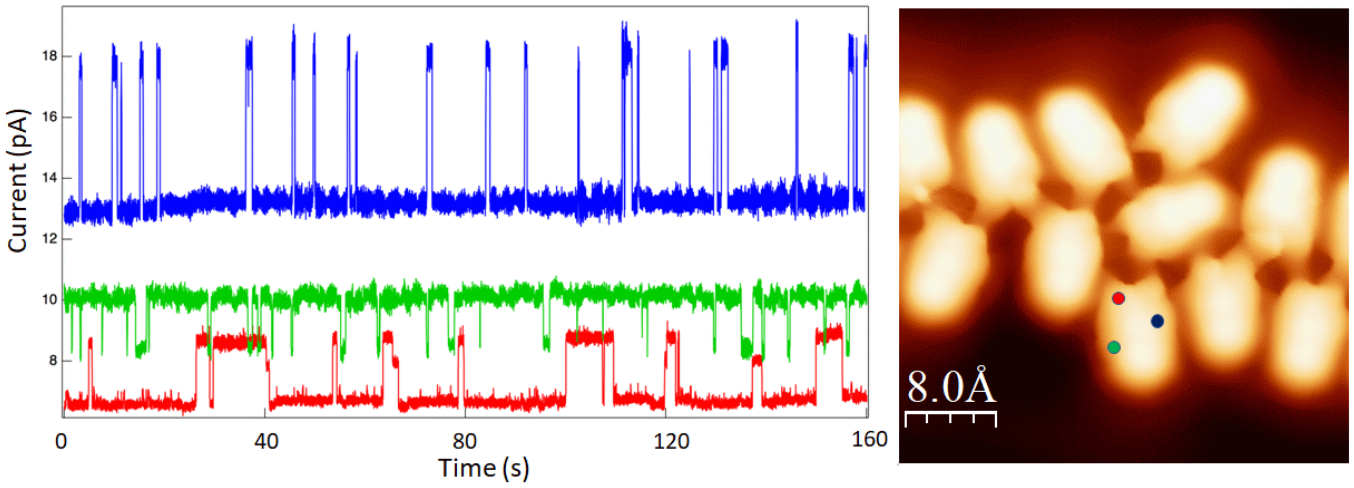

Figure S4. Three telegraph noise traces taken with different tip positioning, as indicated by the coloured circles in the image. The red curve is taken from the same measurement presented in figure 3 of the manuscript (last part of this curve corresponds to the first part of the curve of the manuscript, upon shifting the time scale). As stated in the manuscript, both rate and different level's dominance vary as the tip positioning is changed.

4. DFT calculations: properties of gas phase tautomers

The energies of tautomers in the gas phase and their frontier orbitals are reported in Table S1 and Figure S5, respectively. For simplicity, calculations of orbitals and spectra have been performed for molecules with reflection symmetry with respect to the *xy* plane. These tautomers are referred as TN$_{sym}$. In the case of T1, the tautomer with lowest energy, it has been verified that this symmetry assumption does not significantly affect the results when calculating the orbitals allowing for the distortion of the anthracene backbone. In the following paragraphs it will be shown that the spectroscopy simulations are also weakly affected by this relaxation. The T2$_{sym}$ geometry we considered, with the hydroxyl hydrogen atoms pointing away from the central ketones, represents the stable configuration for this tautomer. In fact, the configuration in which the hydrogen atoms point towards the ketones spontaneously switched to T1$_{sym}$ while performing structural optimization.

Tautomer	**T0$_{(sym)}$**	**T1$_{sym}$**	**T1**	**T2 $_{sym}$**	**T2**	**T3 $_{sym}$**	**T3**
Energy relative to T1 (eV)	0.90	0.09	0	2.10	1.98	1.09	1.01

Table S1. Calculated Total Energy for the four tautomers of Figure 1, in their symmetric form (T*N*$_{sym}$) and in their relaxed form (T*N*). T0 preserves the symmetry after relaxation so T0sym=T0.

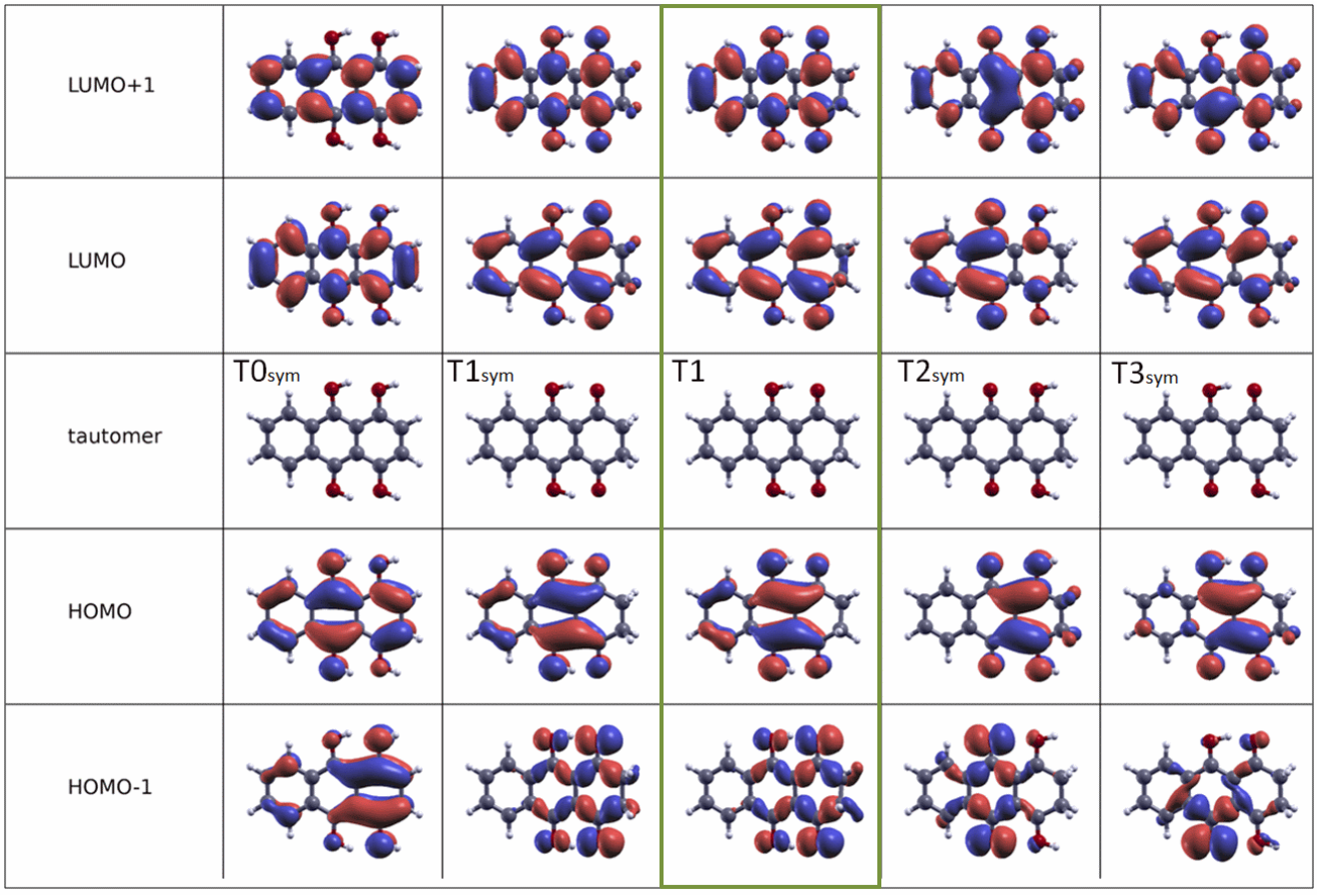

Figure S5. Graphical representation of the first occupied and unoccupied orbitals calculated for the different LQZ symmetric tautomers and for T1.

5. DFT calculations: Spectroscopic assignments

5.1: T1sym vs T1

The presence of the diketo-quinol upon tautomerization promotes the geometrical distortion of the corresponding termination of the anthracene backbone. Figure S6 reports the C1s NEXAFS and XPS calculations for the T1 tautomer in its distorted form (T1) and for the case in which the symmetry of the backbone was forced to be preserved (T1sym). Our findings show that the distortion introduced by the tautomerization poorly affects the spectroscopic properties. The same result was found for O1s (data not shown). For this reason, for simplicity, the calculations of the spectra for the comparison between the different tautomers have been done adopting the symmetric form of the molecules. We remark that the T1 spectra presented in the manuscript are calculated for the most stable distorted case.

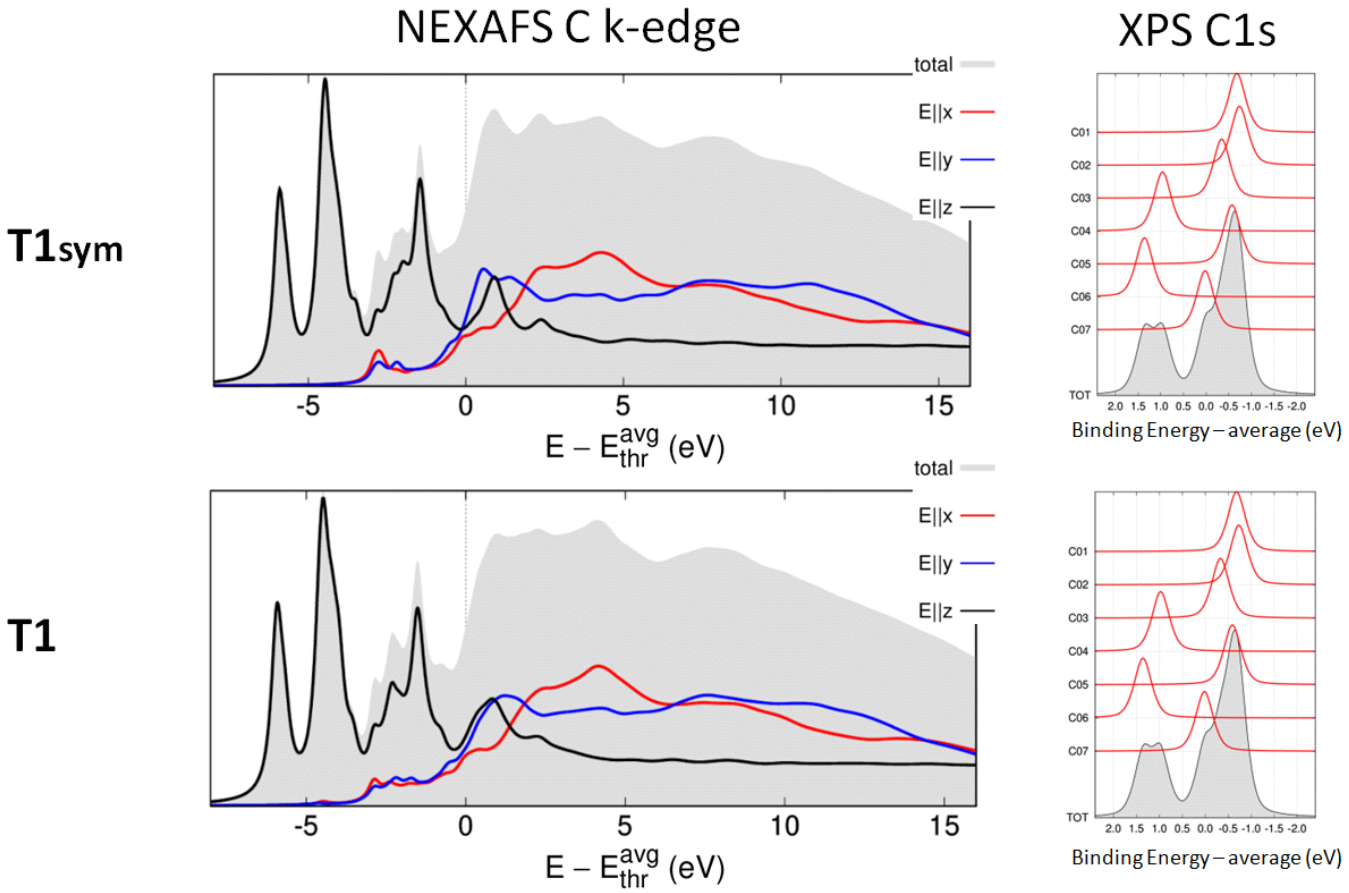

Figure S6. Calculated C1s spectra calculated for the distorted (top) and for the symmetric (bottom) T1 tautomer. The distortion only poorly affects the spectroscopic features on both NEXAFS and XPS spectra.

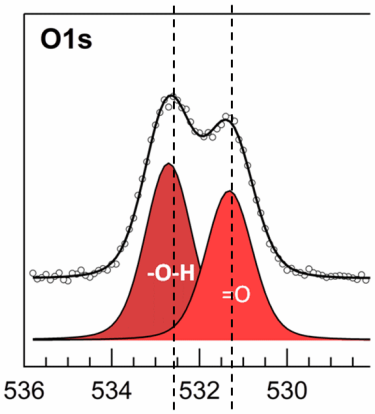

T0sym

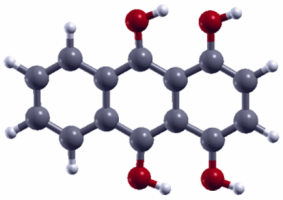

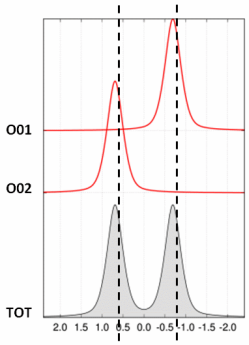

T1sym

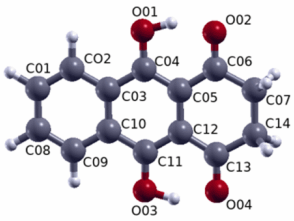

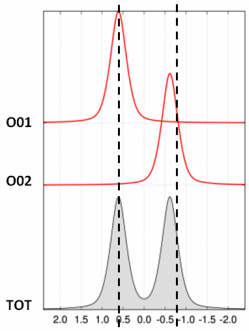

T2sym

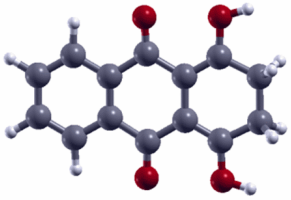

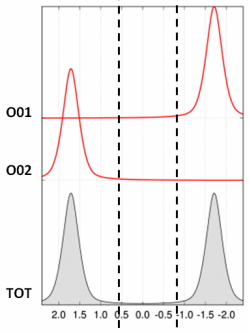

T3sym

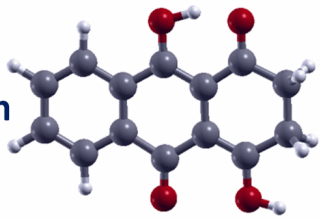

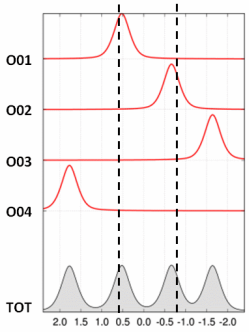

Binding energy – average (eV)

Figure S7. O1s XPS DFT simulated spectra for the T0sym, T1sym, T2sym and T3sym tautomers, compared with the experimental result. The simulated T1sym spectrum matches the experimental one, similarly to the T0sym spectrum. Conversely, features computed for T2sym and T3sym differ significantly from observations.

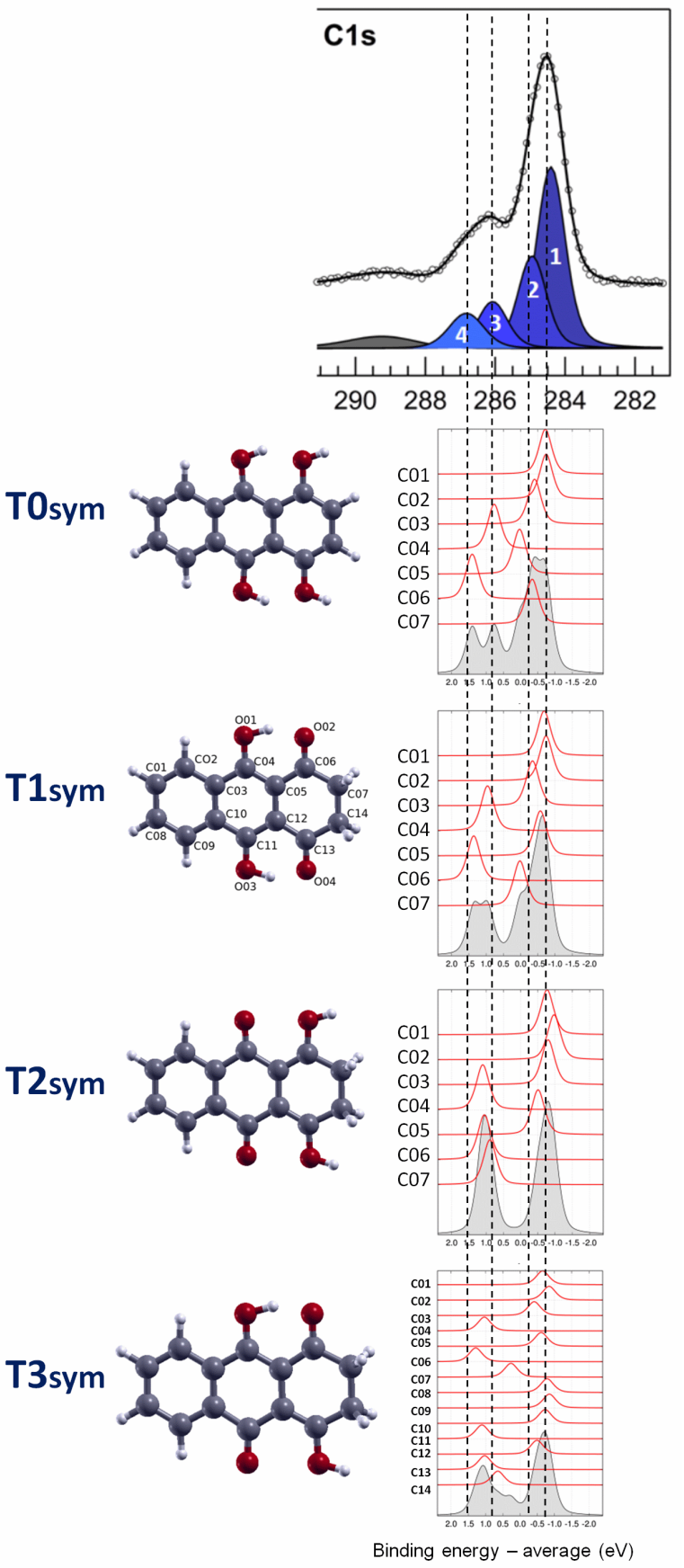

Figure S8. XPS DFT simulated spectra for the T0sym, T1sym, T2sym and T3sym tautomers, compared with the experimental result.

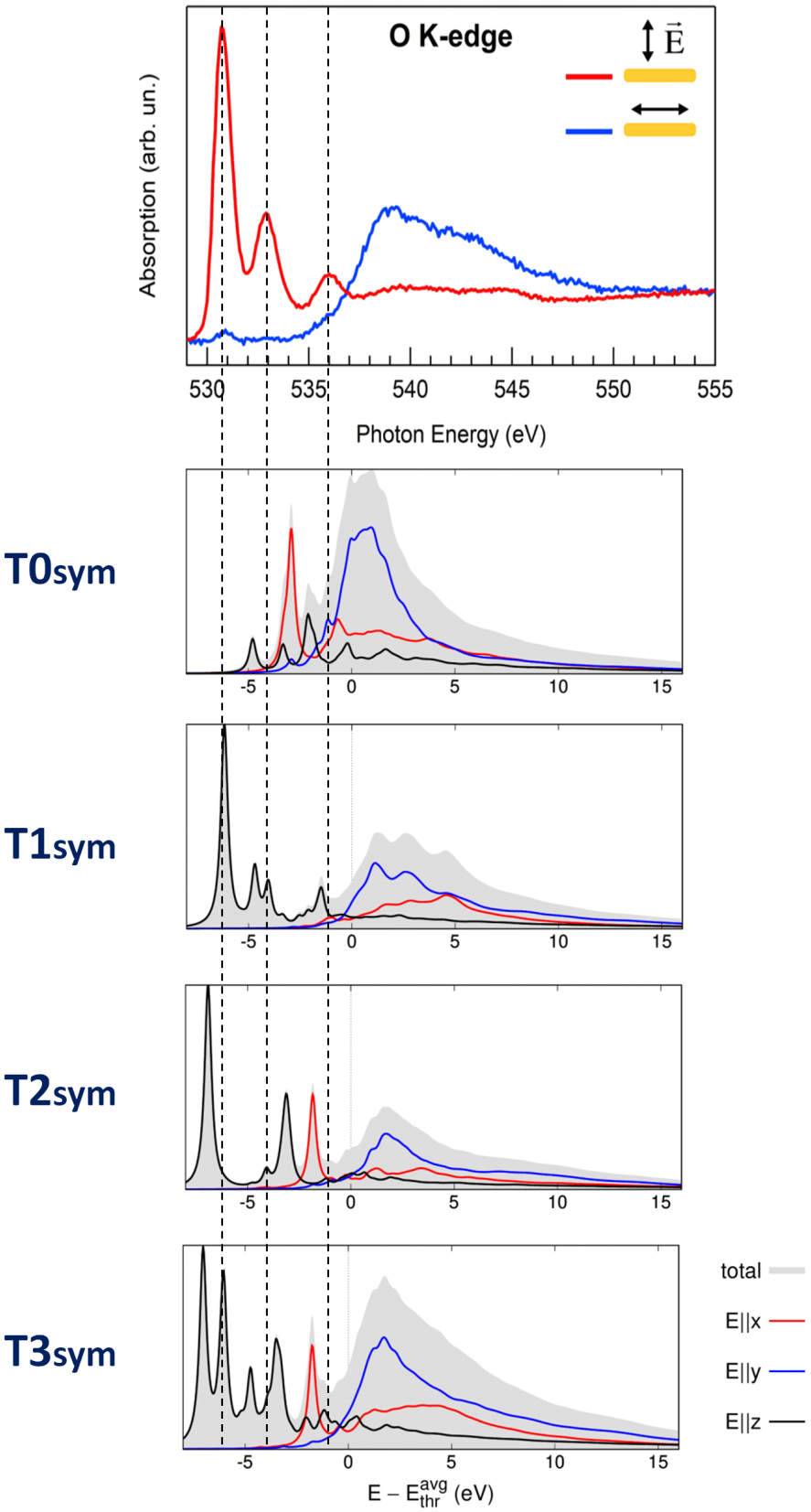

Figure S9 O1s NEXAFS spectra measured (top panel) and simulated for the T0sym T1sym, T2sym and T3sym tautomers (lower panels). T1sym spectrum better agrees with experimental curve with respect to other tautomers, as it properly reproduces the three π* transitions indicated by the dotted black lines, in terms of both relative intensities and position. Energy alignment between theoretical and experimental curve is made by optimizing the overall superposition of the spectral features.

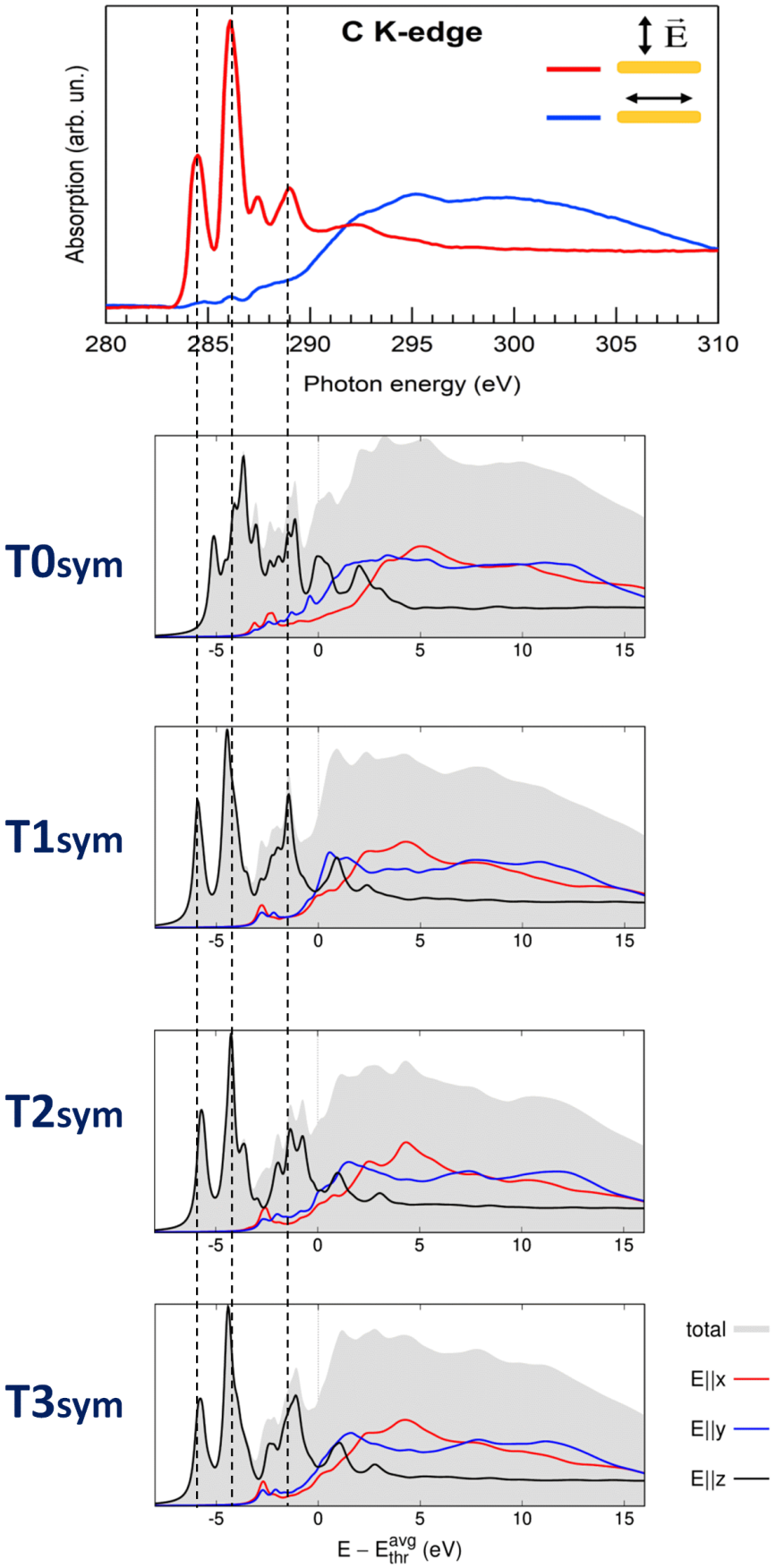

Figure S10 C1s NEXAFS spectra measured (top panel) and simulated for the T0sym, T1sym, T2sym and T3sym tautomers (lower panels). As for O1s, T1sym spectrum better agrees with experimental curve with respect to other tautomers. Energy alignment between theoretical and experimental curve is made by optimizing the overall superposition of the spectral features.

T1 tautomer: C1s Nexafs assignments

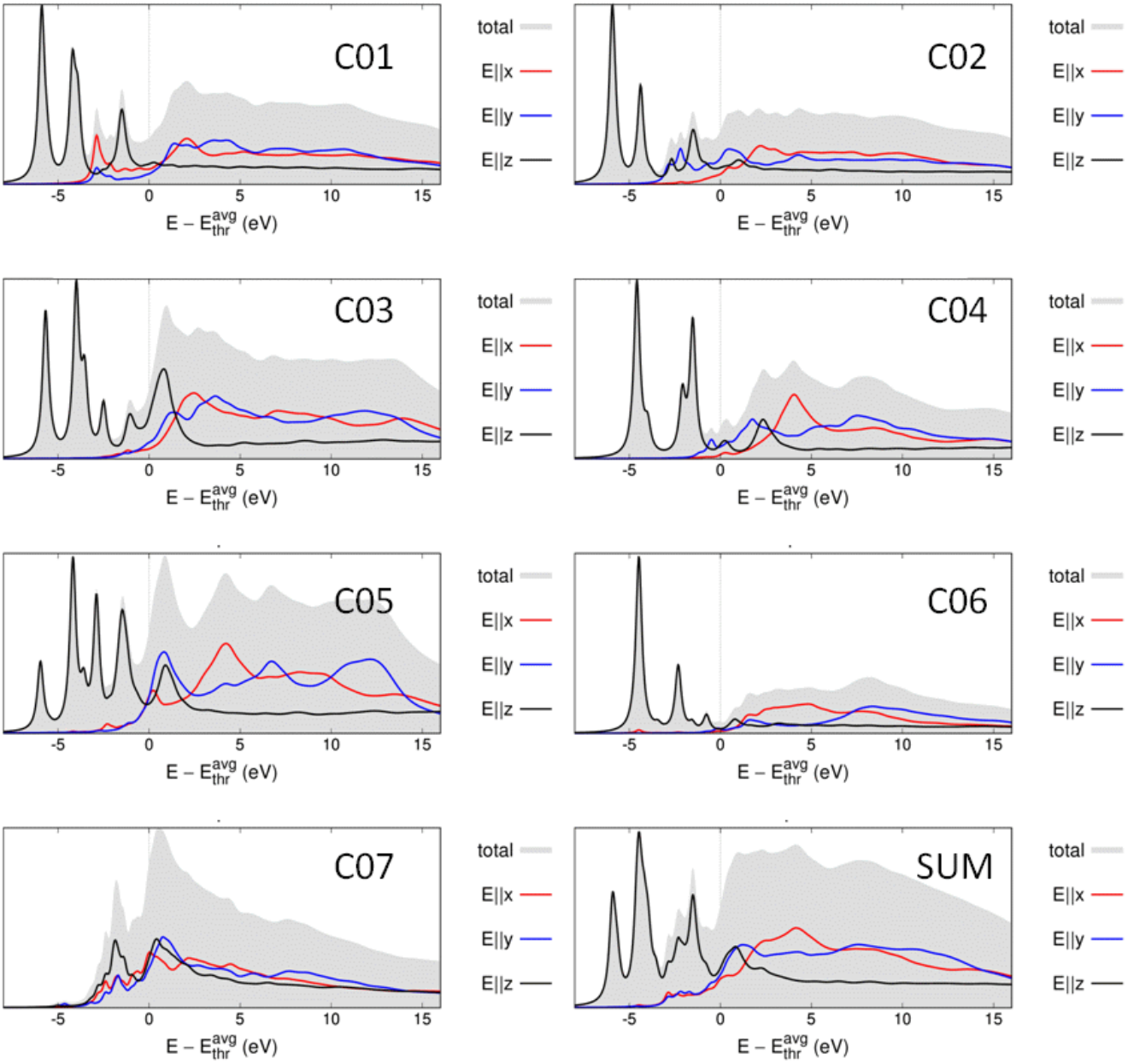

Figure S11 Calculated T1 NEXAFS C1s spectral contributions of the non equivalent carbon atoms. See model in figure S6 for carbon atoms numbering.

6. DFT calculations: Intermolecular hydrogen bonding

In order to describe the intermolecular bonding scheme of the LQZ porous assembly, we built a model for a 2D crystal with 6 molecules / unit cell as inspired by the experimental STM images. The initial molecular coordinates are obtained from the gas phase structure by subsequent 60° rotations around a common axis located at the nanopore, about 10 Å from the center of the molecule. Variable-cell structural relaxations are then used to optimize the in-plane lattice constant and coordinates.

The unit cell of the overlayer contains two trimers (two of them indicated by the green dotted triangles in Figure S11). As a result of the calculations, the lattice constant of the molecular overlayer is 25.8 Å and the bonding energy is of 0.25 eV / cell. Each molecule (all are equivalent by symmetry) has 5 nearest neighbours, pairing in three different ways: (i) with two molecules within the same trimer; (ii) with one molecule lying nearly parallel; (iii) with two molecules facing the same nanopore. The resulting interaction scheme is depicted for one trimer in Fig S11. The coloured arrows identify, by proximity, the molecular terminations involved in the different interactions. In order to estimate the different interaction energies, we calculate the total energy of molecular overlayers where only pairs or trimers of the molecules of the unit cell involved in the considered interaction are included.

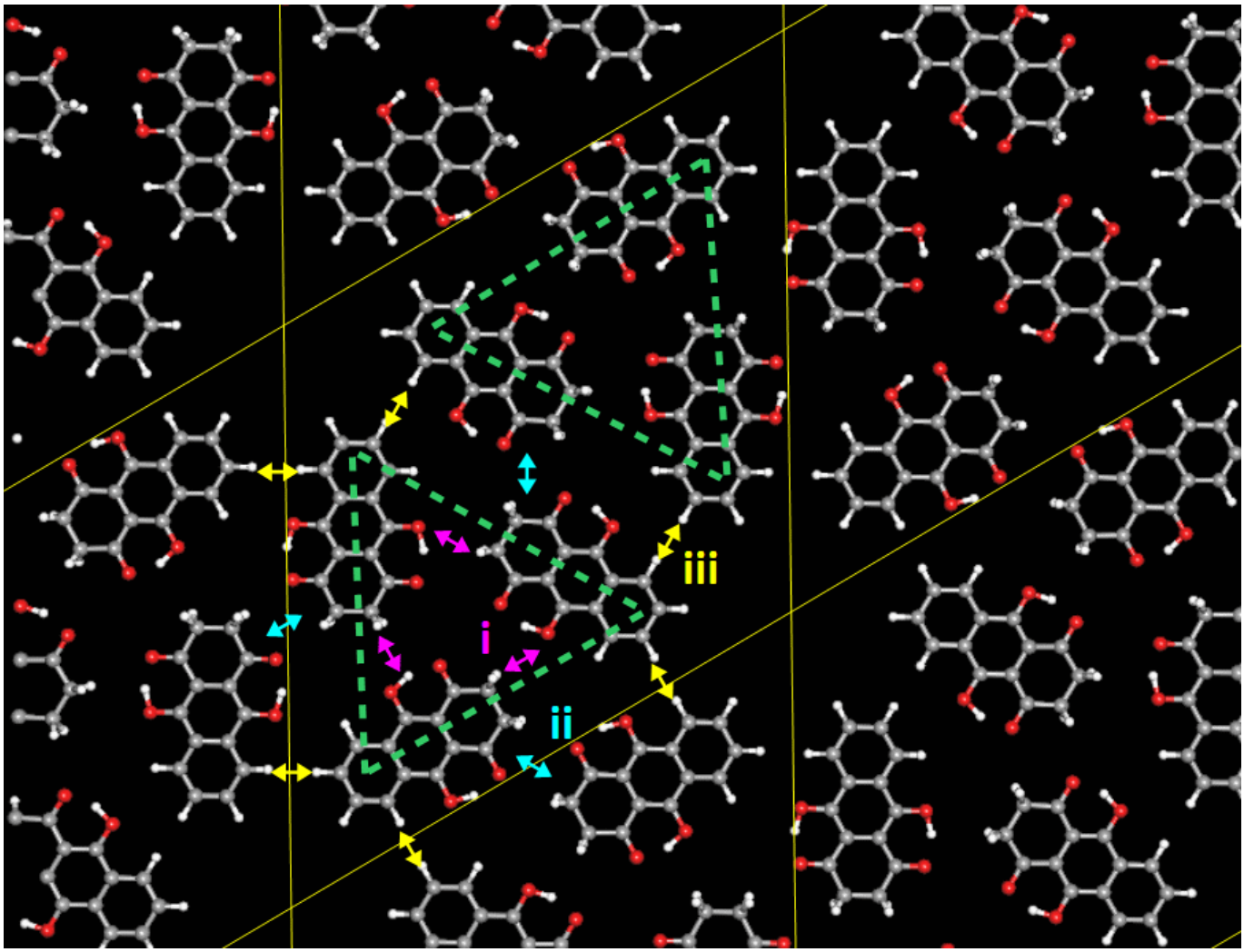

Figure S11. Structure of the molecular overlayer obtained by DFT calculations, by relaxation of the structure suggested by STM images

It results that : the trimers, which when isolated are stabilized by three (i) bonds, have a binding energy of 19 meV; the (iii) interaction in fact does not give any contribution to the bonding energy of the overlayer; the (ii)

bonding between the trimers is 71 meV.

Both (i) and (ii) interactions are related to the oxygen atoms which, as expected play a fundamental role in the assembly process. The strongest intermolecular bond, (ii), is due to the facing of the keto-enolic termination of adjacent molecules. We can speculate that the formation of the trimers is promoted by the symmetry of the substrate and that the high (ii) affinity stabilizes clusters of trimers. On the other hand the (ii) interaction may be seen as a competitor of the trimer formation and lead to less ordered assembly of the LQZ molecules. The low coverage assembly reported in Figure S2 shows both situations, with most of the molecules forming regular chains of pores and part of them assembled in a disordered stripe. We recall however that we are neglecting the interaction of the molecules with the substrate, which could in part modify the relative importance of the different intermolecular interactions.

Bibliography

1 A. Cossaro, L. Floreano, A. Verdini, L. Casalis and A. Morgante, *Phys. Rev. Lett.*, 2009, **103**, 119601.

2 I. Horcas, R. Fernández, J. M. Gómez-Rodríguez, J. Colchero, J. Gómez-Herrero and A. M. Baro, *Rev. Sci. Instrum.*, 2007, **78**.

3 J. P. Perdew, K. Burke and M. Ernzerhof, *Phys. Rev. Lett.*, 1996, 77, 3865–3868.

4 P. Giannozzi, S. Baroni, N. Bonini, M. Calandra, R. Car, C. Cavazzoni, D. Ceresoli, G. L. Chiarotti, M. Cococcioni, I. Dabo, A. Dal Corso, S. de Gironcoli, S. Fabris, G. Fratesi, R. Gebauer, U. Gerstmann, C. Gougoussis, A. Kokalj, M. Lazzeri, L. Martin-Samos, N. Marzari, F. Mauri, R. Mazzarello, S. Paolini, A. Pasquarello, L. Paulatto, C. Sbraccia, S. Scandolo, G. Sclauzero, A. P. Seitsonen, A. Smogunov, P. Umari and R. M. Wentzcovitch, *J. Phys. Condens. Matter*, 2009, **21**, 395502–395520.

5 G. Fratesi, V. Lanzilotto, S. Stranges, M. Alagia, G. P. Brivio and L. Floreano, *Phys. Chem. Chem. Phys.*, 2014, **16**, 14834–14844.

6 G. Fratesi, V. Lanzilotto, L. Floreano and G. P. Brivio, *J. Phys. Chem. C*, 2013, **117**, 6632–6638.

7 E. Pehlke and M. Scheffler, *Phys. Rev. Lett.*, 1993, **71**, 2338–2341.

8 M. Leetmaa, M. P. Ljungberg, A. Lyubartsev, A. Nilsson and L. G. M. Pettersson, *J. Electron Spectros. Relat. Phenomena*, 2010, **177**, 135–157.

9 L. Triguero, L. G. M. Pettersson and H. Ågren, *Phys. Rev. B*, 1998, **58**, 8097–8110.

10 C. Gougoussis, M. Calandra, A. P. Seitsonen and F. Mauri, *Phys. Rev. B - Condens. Matter Mater. Phys.*, 2009, **80**.